Stroke

BASIC AND TRANSLATIONAL SCIENCES

Small Extracellular Vesicles From Hypoxia-Neuron Maintain Blood-Brain Barrier Integrity

Wei Chen, MD*; Yousheng Wu, MD*; Ying Liang, MSc*; Xuanlin Su, MD*; Man Ke, MSc; Die Deng, MD; Jiankun Zang, MD; Jielin Zhu, MSc; Hongcheng Mai, MD, PhD; Anding Xu, MD, PhD; Dan Lu, MD, PhD

BACKGROUND: Acute ischemic stroke disrupts communication between neurons and blood vessels in penumbral areas. How neurons and blood vessels cooperate to achieve blood-brain barrier repair remains unclear. Here, we reveal crosstalk between ischemic penumbral neurons and endothelial cells (ECs) mediated by circular RNA originating from oxoglutarate dehydrogenase (CircOGDH).

METHODS: We analyzed clinical data from patients with acute ischemic stroke to explore the relationship between CircOGDH levels and hemorrhagic transformation events. In addition, a middle cerebral artery occlusion and reperfusion mouse model with neuronal CircOGDH suppression was used to assess endothelial permeability. ECs with increased CircOGDH expression were analyzed for changes in COL4A4 (collagen type IV alpha 4) levels, and in vitro coculture experiments were conducted to examine small extracellular vesicle–mediated CircOGDH transfer between neurons and ECs.

RESULTS: Clinical data indicated that reduced CircOGDH levels were correlated with increased hemorrhagic transformation in patients with acute ischemic stroke. In the middle cerebral artery occlusion and reperfusion model, neuronal CircOGDH suppression impaired the restoration of endothelial permeability. ECs with increased CircOGDH expression exhibited higher COL4A4 levels, which helped maintain vascular stability. In vitro, hypoxic neurons transferred CircOGDH to ECs via small extracellular vesicles, leading to elevated COL4A4 expression and enhanced endothelial integrity.

CONCLUSIONS: Our findings highlight the significance of CircOGDH in neuron-EC crosstalk via small extracellular vesicles in the ischemic penumbra, emphasizing the need for balanced intervention strategies in acute ischemic stroke management.

GRAPHIC ABSTRACT: A graphic abstract is available for this article.

Key Words: blood-brain barrier ■ circular RNA ■ endothelial cells ■ ischemic stroke ■ neurovascular coupling

The primary goal of therapeutic interventions for acute ischemic stroke (AIS) is to rescue hypoxic neurons in the penumbra.[1,2] Recent advancements have identified circular RNA originating from oxoglutarate dehydrogenase (CircOGDH), a hypoxia-induced high expression in neurons circular RNA, as a crucial target for alleviating neuronal hypoxia in penumbral regions.[3] While rescuing neurons in these areas is essential, maintaining adequate blood oxygen levels for penumbral hypoxia recovery relies on proper blood supply via neurovascular coupling[4,5] Recent evidence underscores the pivotal role of penumbra hypoxic neurons in neurovascular communication,[6,7] as CircOGDH, originating from these neurons, interacts not only within neurons but also with the

Correspondence to: Dan Lu, MD, PhD, Department of Neurology and StrokeCenter, The First Affiliated Hospital of Jinan University, Guangzhou, Guangdong 510632, China, Email ludan@jnu.edu.cn; Anding Xu, MD, PhD, Department of Neurology and Stroke Center, The First Affiliated Hospital of Jinan University, Guangzhou, Guangdong 510632, China, Email tlil@jnu.edu.cn; or Hongcheng Mai, MD, PhD, Department of Neurology, Sun Yat-sen Memorial Hospital, Sun Yat-sen University, Guangzhou, China, Email maihch7@mail.sysu.edu.cn
*W. Chen, Y. Wu, Y. Liang, and X. Su contributed equally.
Supplemental Material is available at https://www.ahajournals.org/doi/suppl/10.1161/STROKEAHA.124.048446.
For Sources of Funding and Disclosures, see page 1579.

Nonstandard Abbreviations and Acronyms

AAV	adeno-associated virus
AIS	acute ischemic stroke
BBB	blood-brain barrier
CircOGDH	circular RNA originating from oxoglutarate dehydrogenase
COL4A4	collagen type IV alpha 4
EC	endothelial cell
H/R	hypoxia/reoxygenation
HBMEC	human brain microvascular endothelial cell
HT	hemorrhagic transformation
MCAO/R	middle cerebral artery occlusion and reperfusion
sEV	small extracellular vesicle
TJ	tight junction

blood-brain barrier (BBB) and is released into circulation. This suggests that solely targeting penumbra CircOGDH in neurons may overlook critical aspects of neural-BBB recovery and coupling. However, the intricate mechanisms through which penumbra CircOGDH affects BBB function in cell-cell communication under hypoxic conditions remain largely unexplored.

Within the central nervous system, cell-cell communication is facilitated by small extracellular vesicles (sEVs).[4,8] Recent studies on neurovascular coupling have highlighted neuron-derived sEVs as carriers of bioactive molecules such as RNAs, including miRNAs and circRNAs, potentially facilitating interactions with BBB endothelial cells (ECs).[9–12] Our prior investigation revealed that hypoxic neuronal sEVs release CircOGDH, influencing downstream extracellular matrix–related proteins such as COL4A4 (collagen type IV alpha 4).[3] This suggests that neuron-derived sEVs might transport CircOGDH to the BBB during hypoxic stress, modulating brain vascular integrity.

This study aimed to investigate the association between CircOGDH levels and poststroke hemorrhagic transformations (HTs) in patients with AIS to understand the link between CircOGDH and BBB integrity. In addition, we assessed the impact of inhibiting CircOGDH on BBB function using a mouse stroke model. Furthermore, in vitro studies have allowed us to investigate the impact of hypoxic neurons on EC function, providing additional insight into the interaction between neurons and ECs.

METHODS

The data that support the findings of this study are available from the corresponding author upon reasonable request. Methodological details beyond the description in the following are provided in the Supplemental Material.

Human Plasma Collection

Patients with AIS with or without HT were recruited from the Department of Neurology and Stroke Center, First Affiliated Hospital of Jinan University, from August 2020 to February 2021 (ethics approval number: KY-2022-205). AIS was confirmed by magnetic resonance imaging, and HT was confirmed by computed tomography. Eighteen patients with AIS without HT were matched with patients with AIS with HT by age, sex, and infarction size. Noncerebrovascular disease controls were also included. Blood samples were collected in ethylenediaminetetraacetic acid (EDTA)-coated tubes, centrifuged at 3000*g* for 15 minutes at 4 °C within 1 hour, and plasma was stored at −80 °C for RNA extraction. Clinical details are presented in Table S9.

Human Brain Tissue Samples

Brain tissue samples were collected from patients with AIS+HT or spontaneous intracerebral hemorrhage. The inclusion criteria for AIS and spontaneous intracerebral hemorrhage were the same as for plasma collection. All procedures were approved by the Medical Ethics Committee of Jinan University (KY-2022-205).

Determination of Penumbra Size

HT was evaluated using computed tomography scans, and hematoma volume was calculated using 3D Slicer software. Hematoma regions were identified and quantified by thresholding, with analysis performed by a blinded investigator.

Immunohistochemistry

Paraffin-embedded brain sections were incubated with primary antibodies (Table S2) and visualized using the poly-horseradish peroxidase (HRP) Anti-Rabbit/Mouse IgG Detection System (Elabscience).

Animals

Adult male C57BL/6J mice (6–8 weeks old, 20–24 g) were housed in a temperature- and humidity-controlled environment with free access to food and water. All procedures adhered to ARRIVE guidelines (Animal Research: Reporting of In Vivo Experiments)[13] and were approved by the Experimental Animal Ethics Committee of Jinan University (project ID: 0201028-03).

Middle Cerebral Artery Occlusion and Reperfusion

Middle cerebral artery occlusion surgery was performed as described previously,[14] always within consistent daytime hours. Mice were anesthetized with isoflurane, and the left middle cerebral artery was occluded with a silicone-coated nylon filament for 60 minutes. After reperfusion, the skin was sutured, and the animals were allowed to recover. The operation time was always maintained between 9 AM and 12 AM.

AAV Construction and Microinjection

Neuron-specific adeno-associated virus (AAV)-human synapsin I promoter (hSyn)-EGFP-shRNA-CircOGDH and AAV-hSyn-EGFP-shRNA-CircCtrl were constructed by Brainvta

 Stroke. 2025;56:1569–1580. DOI: 10.1161/STROKEAHA.124.048446

(Wuhan, China). Mice were microinjected with 2 µL of AAV (1×10^{10} vg/µL) into the left lateral ventricle. After 21 days, mice were assigned to groups for middle cerebral artery occlusion and reperfusion (MCAO/R) surgery.

Magnetic Resonance Imaging

Mice underwent a magnetic resonance imaging using a 9.4T scanner. Diffusion-weighted imaging and fluid-attenuated inversion recovery were performed at 3 and 24 hours post-middle cerebral artery occlusion. Quantitative analysis of diffusion-weighted imaging and fluid-attenuated inversion recovery was conducted using ImageJ and RadiAnt software. Infarct volumes were calculated using the modified ABC/2 method.[3]

Prussian Blue Staining

Prussian blue staining was performed to detect iron in brain sections. Sections were incubated with potassium ferrocyanide, washed, and counterstained with Nuclear Fast Red.

BBB Integrity

BBB permeability was assessed using 2% Evans blue dye injected into the tail vein. After 1 hour, mice were perfused with PBS, and brain tissue was homogenized for spectrophotometric measurement at 620 nm. Sulfo-N-hydroxy succinimide (NHS)-biotin perfusion and immunofluorescence with streptavidin-fluorescein isothiocyanate (FITC) were used to assess BBB integrity in frozen brain sections.

Transmission Electron Microscopy

Brain samples from the ischemic penumbra were fixed in glutaraldehyde and processed for transmission electron microscopy to assess ultrastructural changes in the BBB.

Cell Cultures and Treatments

SH-SY5Y neuroblastoma cells and human brain microvascular ECs (HBMECs; https://www.atcc.org/products/crl-3245) were cultured in Dulbecco's Modified Eagle Medium/Nutrient Mixture F-12 (DMEM/F-12) with 10% fetal bovine serum (FBS) and 1% penicillin-streptomycin. Cells were exposed to hypoxic conditions for 3 hours in a hypoxia chamber and then returned to normoxic conditions for reoxygenation.

Western Blotting

Proteins were extracted using radio immunoprecipitation assay lysis buffer (RIPA) buffer, separated by SDS-PAGE, and transferred to nitrocellulose membranes. Membranes were incubated with primary antibodies (eg, COL4A4, β-actin, CD34, and CD63) followed by horseradish peroxidase (HRP)-conjugated secondary antibodies. Chemiluminescence was used for detection.

Quantitative Reverse Transcription Polymerase Chain Reaction

RNA was extracted from cells, sEVs, and brain tissues using TRIzol. Reverse transcription was performed using PrimeScript RT Master Mix (Takara). Quantitative reverse transcription polymerase chain reaction was conducted using SYBR Green (Roche) and analyzed with the $2^{-\Delta\Delta CT}$ method.

sEV Isolation and Characterization

sEVs were isolated from cell culture supernatants and plasma using ultracentrifugation or polymer precipitation. sEVs were characterized by transmission electron microscopy and nanoparticle tracking analysis.

Statistical Analysis

Data were analyzed using SPSS (Windows, version 27.0) or GraphPad Prism 8.01. For $n<6$, nonparametric tests were used. For normally distributed data, the Student *t* test or ANOVA was applied. Significance was set at $P<0.05$.

RESULTS

Blood CircOGDH Levels Are Negatively Correlated With HT After Stroke in Patients

To explore the association between CircOGDH and the BBB, we conducted a matched observational case-control study involving 18 patients with AIS within 24 hours of onset, with and without hemorrhage (Figure 1A and 1B). Our analysis revealed that CircOGDH expression in plasma was lower in patients with AIS with HT than in those without HT (Figure 1C). Interestingly, we observed a negative correlation between CircOGDH levels and hematoma volume in patients with AIS with HT (lower CircOGDH levels with higher hematoma volume; Figure 1D; correlation coefficient r=−0.629; $P=0.014$). Furthermore, to investigate the specificity of CircOGDH expression related to hypoxia-induced HT, we compared CircOGDH staining in human brain tissues from patients with AIS with HT and from patients with spontaneous intracerebral hemorrhage without hypoxia. CircOGDH expression was ≈4× higher than in tissues from patients with AIS with HT (Figure 1E and 1F). The relationship between hypoxia-related neuronal CircOGDH and HT in patients with AIS suggests a potential influence of CircOGDH on BBB integrity.

Reduced Hypoxic Neuronal CircOGDH Levels Result in Higher BBB Permeability Following Ischemic Stroke in Mice

Building on previous evidence suggesting that inhibiting neuronal CircOGDH could enhance stroke outcomes,[3] we administered an AAV-mediated CircOGDH knockdown with neuron-specific targeting using the human synapsin I promoter (hSyn) into the lateral ventricle of mice following middle cerebral artery occlusion surgery and reperfusion for 24 hours (Figure 2A). Baseline cerebral blood flow measurements showed no significant differences between the sham, $hSyn^{sh\_CircCtrl}$, and $hSyn^{sh\_CircOGDH}$ groups (Figures S1 and S2). Our analyses showed reduced CircOGDH expression in the ischemic brain of $hSyn^{sh\_CircOGDH}$ mice compared with that of $hSyn^{sh\_CircCtrl}$ mice, confirmed by fluorescence in situ hybridization staining (Figure 2B and 2C) and quantitative

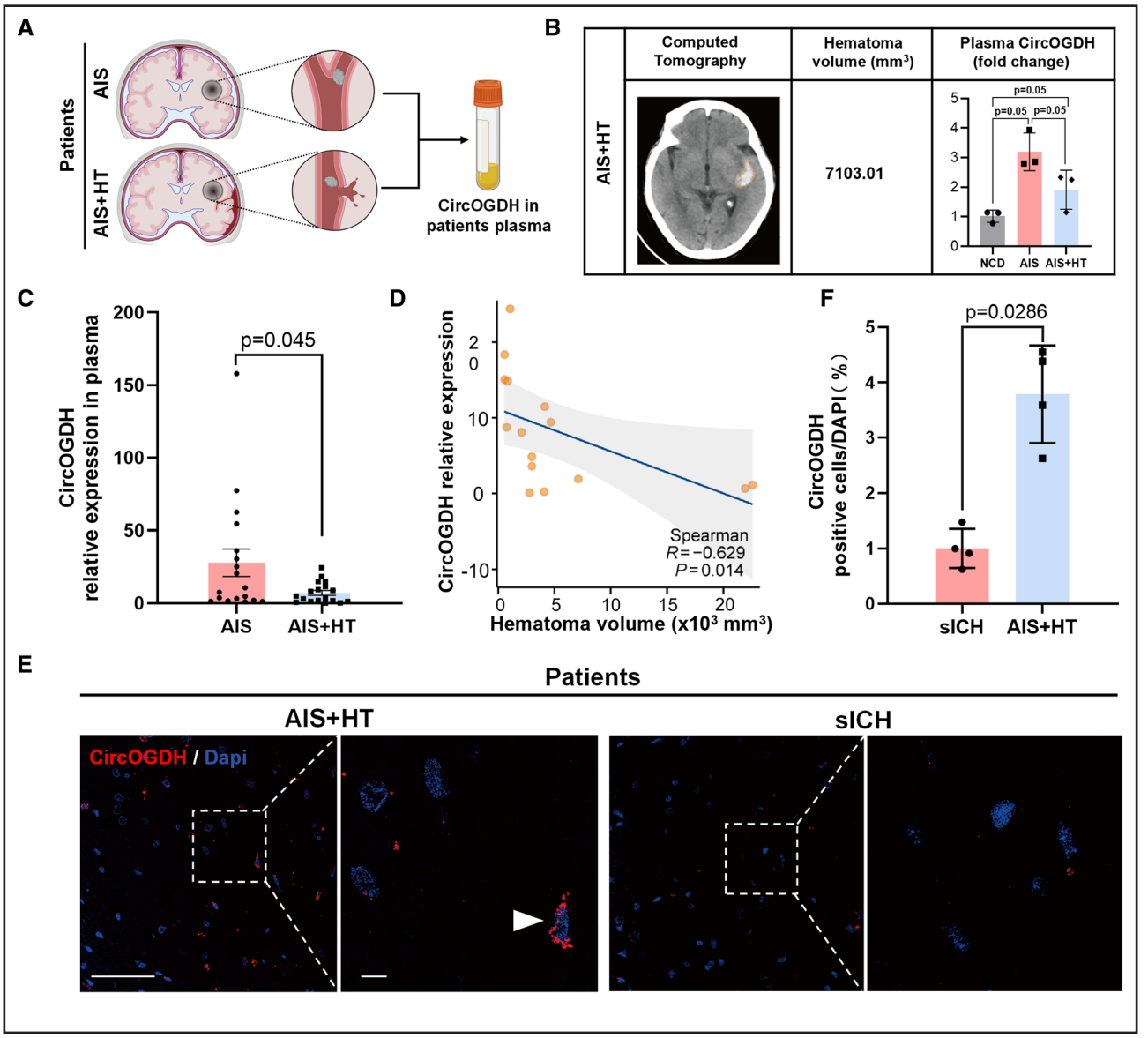

Figure 1. Lower circular RNA originating from oxoglutarate dehydrogenase (CircOGDH) expression in patients with acute ischemic stroke (AIS) with hemorrhage compared with those without hemorrhage.

A, Experimental scheme for identifying CircOGDH in the plasma of patients. Patients with AIS with hemorrhagic transformation (HT) and patients with AIS without HT were used to identify the relationship between CircOGDH and HT. Created in BioRender. **B**, Representative data from a patient with AIS with HT showing computed tomography (CT) images and relative CircOGDH expression levels (fold change). High-density areas (highlighted by yellow dashed lines) in CT images indicate the presence of hemorrhagic regions, with hematoma volume calculated using 3D Slicer software. The histogram depicts relative CircOGDH expression in patients with AIS with HT on the day of CT diagnosis of HT (day 1 of onset) compared with patients with AIS without HT (day 1) and those with noncerebrovascular disease (NCD; n=1). Data are presented as means±SD, nonparametric tests with the Mann-Whitney *U* test. **C**, Quantitative reverse transcription polymerase chain reaction of CircOGDH expression levels in the plasma of patients with AIS with or without HT (n=18) on the day of CT diagnosis of HT (within 24 hours). Data are presented as means±SEM; the Student *t* test was used. **D**, Spearman correlation between hematoma volume and CircOGDH expression levels in 15 patients with AIS with HT, controlled for age, sex, and TOAST criteria (Trial of ORG 10172 in Acute Stroke Treatment), partial correlation coefficient (r=−0.629; *P*=0.014). **E** and **F**, Images of CircOGDH (red) and their quantification (integrated optical density) in spontaneous intracerebral hemorrhage (sICH) and patients with AIS+HT (n=4). Nuclei were stained with 4′,6-diamidino-2-phenylindole (DAPI). Scale bar, 20 μm. Data are presented as means±SD (**F**); the Mann-Whitney *U* test was used.

reverse transcription polymerase chain reaction (Figure 2D). Although CircOGDH is conserved in hypoxic neurons and linked to their survival in the penumbra, our analysis of neuronal nuclear antigen expression in brain tissue proteins showed no significant difference in neuronal nuclear antigen levels within the infarct core between the hSyn^{sh_CircOGDH} and hSyn^{sh_CircCtrl} groups. However, in the ischemic penumbra, the hSyn^{sh_CircOGDH} group exhibited a notable increase in neuronal nuclear antigen expression by at least 1.4-fold (Figure S3).

 Stroke. 2025;56:1569–1580. DOI: 10.1161/STROKEAHA.124.048446

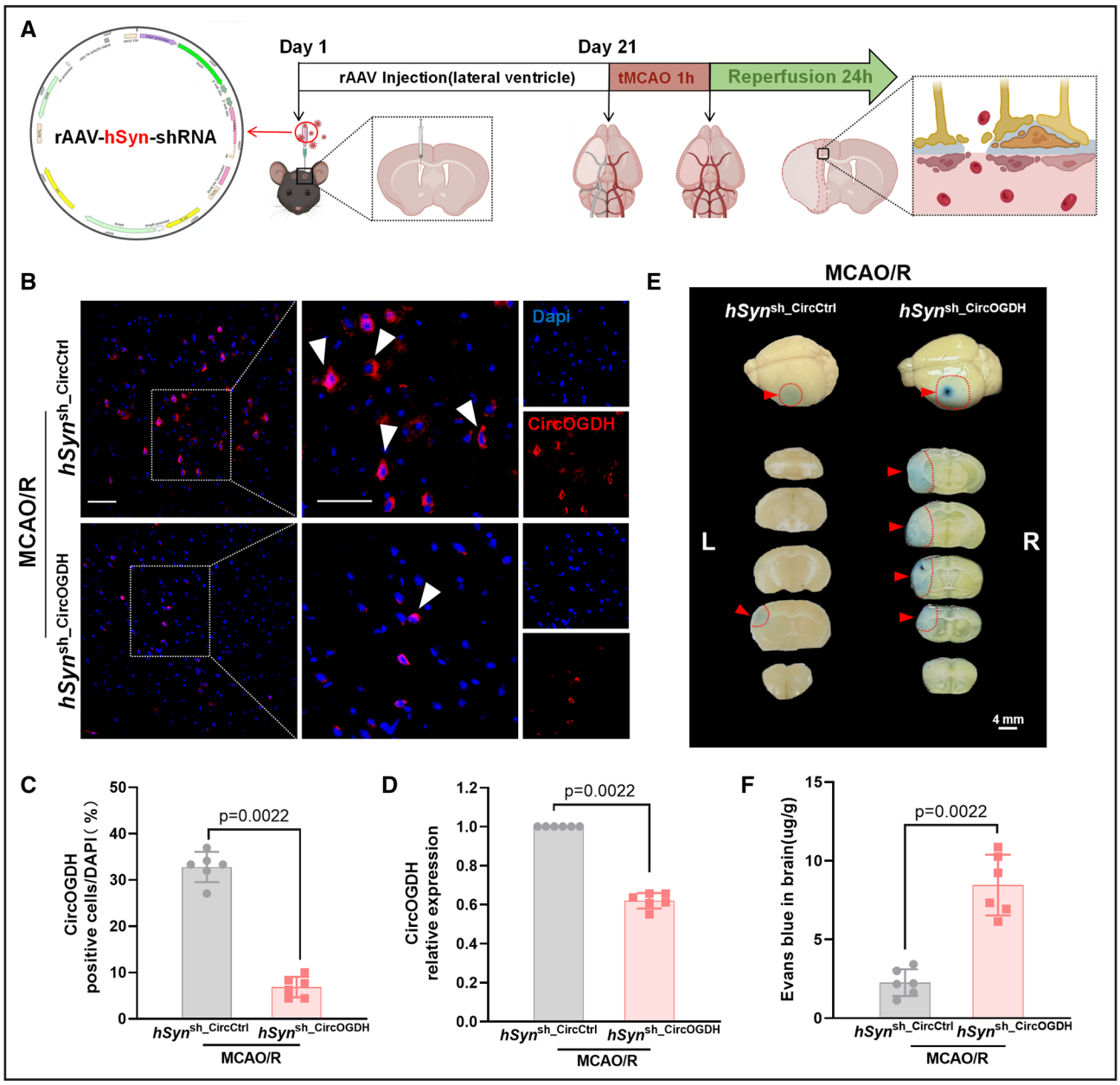

Figure 2. Deficiency of neuronal circular RNA originating from oxoglutarate dehydrogenase (CircOGDH) exacerbates blood-brain barrier (BBB) permeability following middle cerebral artery occlusion and reperfusion (MCAO/R).
A, Schematic illustration of the experimental procedure in mice. Neuron-specific knockdown of CircOGDH was achieved by administering adeno-associated virus (AAV)-hSyn^{sh_CircOGDH} into the lateral ventricles of the mice, with expression in the brain tissue after 21 days. Subsequently, the mice underwent middle cerebral artery occlusion (MCAO) for 1 hour, followed by a 24-hour reperfusion. The brains were then harvested after various treatments. Created in BioRender. **B** and **C**, Fluorescence in situ hybridization (FISH) showing CircOGDH localization (red) in the penumbra tissue (PEN; n=6). Scale bar, 20 μm. **D**, Quantitative reverse transcription polymerase chain reaction analysis of CircOGDH abundance in PEN tissues of mouse brains (n=6). **E** and **F**, Representative image showing Evans blue extravasation throughout the mouse brain, with red arrows indicating areas of leakage. Scale bar, 4 mm. Data are presented as means±SD; the Student *t* test (**C**, **D**, and **F**) was used.

In addition, the hSyn^{sh_CircOGDH} group showed a 10% reduction in infarct size compared with the hSyn^{sh_CircCtrl} group (Figure S4), indicating a modest improvement in cerebral infarct size and partial mitigation of neuronal injury in the ischemic penumbra following targeted CircOGDH knockdown. However, consistent with clinical data, lower neuronal CircOGDH levels were associated with BBB damage and an increased HT rate. Specifically, we observed increased Prussian blue staining (1.62±0.16-fold; Figure S5), Evans blue intensity (3.74±0.38-fold; Figure 2E and 2F), and NHS-biotin leakage (3.25±0.29-fold; Figure S6) in the hSyn^{sh_CircOGDH} group compared with the hSyn^{sh_CircCtrl} group. These findings suggest that targeted CircOGDH knockdown affects the biological homeostasis of the neurovascular unit under hypoxic conditions.

Inhibition of Neuronal CircOGDH Leads to Lower Expression of Tight Junction (TJ) Proteins and Changes in BBB Structure After MCAO/R

To explore the impact of reduced neuronal CircOGDH on BBB permeability, we investigated its relationship with BBB component proteins, specifically TJ proteins. Immunofluorescence staining of mouse brains after MCAO/R revealed decreased expression of zonula occludens-1 (ZO-1) and occludin in the hSyn^{sh_CircOGDH} group compared with the hSyn^{sh_CircCtrl} group (Figure 3A and 3B). This reduction was further confirmed by the Western blot analysis, which showed an average 31% decrease in ZO-1, a 15% decrease in occludin, and a 12% decrease in claudin-5 expression in the ischemic penumbra of the hSyn^{sh_CircOGDH} group (Figure 3C and 3D). Moreover, there was no significant difference in CD105 and CD34 protein expression, indicating no major changes in angiogenesis between the 2 groups in either the core or penumbra region (Figure S7).

To assess the effects of CircOGDH on BBB ultrastructure after ischemic stroke, we examined EC gaps using transmission electron microscopy (Figure 3E). The hSyn^{sh_CircOGDH} group exhibited clear gaps in the BBB structure (indicated by red arrows), while the hSyn^{sh_CircCtrl} group displayed fewer disruptions in TJs. The hSyn^{sh_CircOGDH} group showed a higher proportion of TJs with gaps, averaging ≈21%, with each TJ strand containing >10 gaps (Figure 3F).

Inhibition of Neuronal CircOGDH Leads to Increased Transcytosis and Endocytosis in BBB ECs in the Mouse Brain After MCAO/R

The role of CircOGDH in regulating transcytosis and endocytosis, contributing to increased BBB

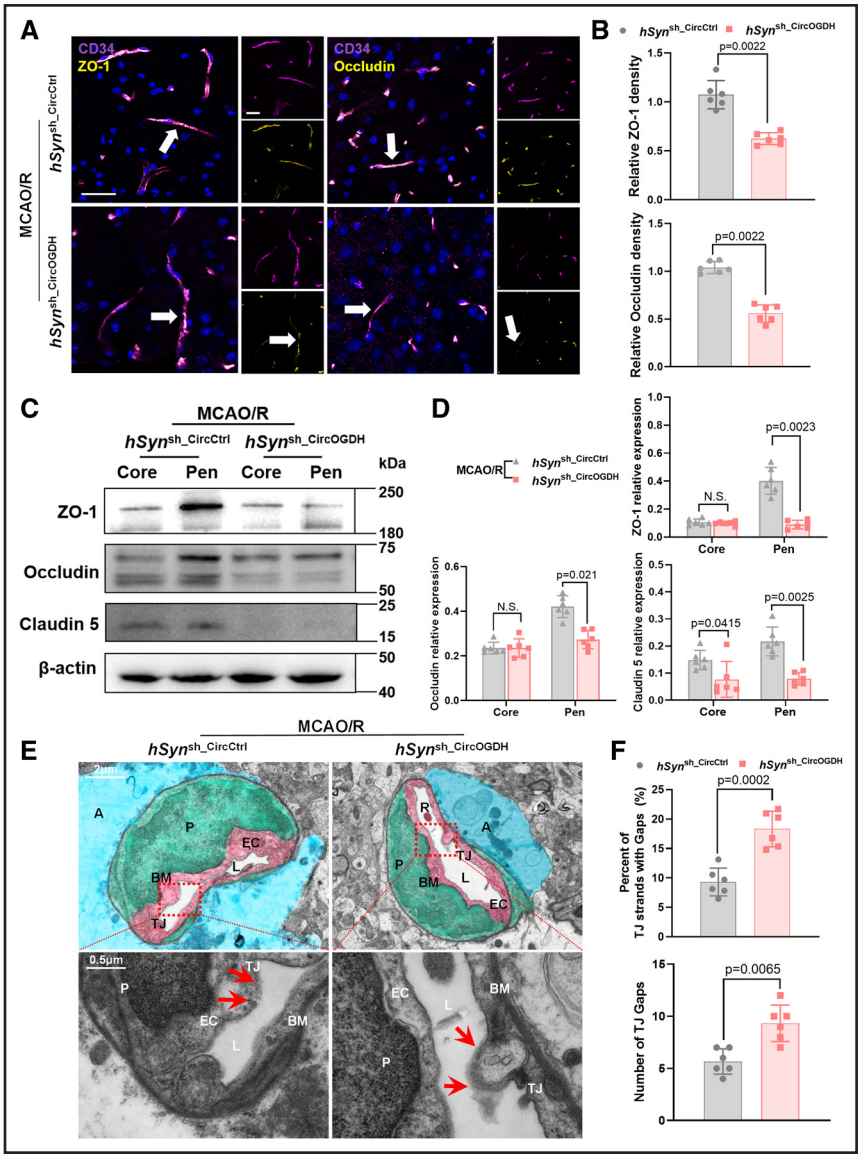

Figure 3. Circular RNA originating from oxoglutarate dehydrogenase (CircOGDH) regulates TJ (tight junction) expression in the blood-brain barrier (BBB) after middle cerebral artery occlusion and reperfusion (MCAO/R).
A and **B**, Protein levels of zonula occludens-1 (ZO-1; yellow; **left**) and occludin (yellow; **right**) were determined using immunofluorescence (IF; **A**) in the penumbra tissue (PEN) of MCAO/R mice (n=6), quantified by measuring ZO-1 and occludin IF signal density normalized by CD34 (magenta) signal area. Scale bar, 20 μm. **C** and **D**, Representative image and statistical analysis of the Western blot for the expression of ZO-1, occludin, and claudin-5 in the PEN and core of MCAO/R mice (n=6). **E**, Transmission electron microscopy image of the BBB in MCAO/R mice. The red box highlights typical TJ gaps. Structurally abnormal TJs containing large gaps are indicated by red arrows. **F**, Statistical analysis of **E**, showing the fraction of TJ strands with gaps, and the number of TJ gaps (n=6). Data are presented as means±SD; the Student *t* test (**B** and **D**) or the Mann-Whitney *U* test (**F**) was used. A (blue) indicates astrocyte end foot; BM, basement membrane; EC (red), endothelial cell; L, lumen; P (green), pericyte; and R, red blood cell.

Stroke. 2025;56:1569–1580. DOI: 10.1161/STROKEAHA.124.048446

permeability after ischemic stroke, remains unexplored. We measured caveolin-1[15,16] and albumin-Alexa594[17] uptake to assess transcytosis and endocytosis (Figure S8). The Western blot analysis revealed significantly higher caveolin-1 expression in the penumbra of the $hSyn^{sh\_CircOGDH}$ group than in the $hSyn^{sh\_CircCtrl}$ group (Figure S9). Immunofluorescence staining also showed a 2.66±1.23-fold increase in caveolin-1 abundance in the $hSyn^{sh\_CircOGDH}$ group (Figure S10). Subsequently, we administered 1% Alb-Alexa594 to examine endocytosis levels. Our findings showed a higher proportion of positive cells in the $hSyn^{sh\_CircOGDH}$ group than in the $hSyn^{sh\_CircCtrl}$ group (18% versus 9.5%; Figure S11). These results suggest that reduced neuronal CircOGDH leads to upregulated EC endocytosis and transcytosis, contributing to impaired BBB function during reperfusion.

Neuronal CircOGDH Delivered to HBMECs via sEVs Increases HBMEC Survival by Elevating CircOGDH Levels After H/R Injury

Previous studies have shown that CircOGDH is enriched in sEVs and released into the bloodstream as a biomarker.[3] We analyzed CircOGDH levels in plasma and plasma sEVs from ischemic stroke mice. In the $hSyn^{sh\_CircOGDH}$ group, CircOGDH levels in plasma were ≈30% of those in the $hSyn^{sh\_CircCtrl}$ group, while levels in plasma sEVs in the $hSyn^{sh\_CircCtrl}$ group were 50% of those in the $hSyn^{sh\_CircOGDH}$ group (Figure 4A). Because neuronal CircOGDH likely facilitates intercellular communication within the neurovascular unit via sEVs, we delivered neuronal sEVs to ECs and examined CircOGDH expression changes in HBMECs. We conducted experiments using HBMECs and SH-SY5Y (neurons) cells cultured separately after 3 hours of hypoxia and 24 hours of reoxygenation, which induced elevation in CircOGDH expression in SH-SY5Y cells (Figure S12). Later setting the coculture system, CircOGDH expression in HBMECs increased by 1.705±0.245-fold. However, when using the sEV inhibitor GW4869 in neuronal regions, CircOGDH levels did not increase in HBMECs after hypoxia/reoxygenation (H/R; Figure 4B).

We further confirmed the uptake of extracted hypoxic SH-SY5Y sEVs in HBMECs over 24 hours using live cell monitoring (Figure 4C). Hypoxia-induced sEVs were collected (Figure S13) from SH-SY5Y cells treated with GW4869 (sEV inhibitor), CircOGDH overexpression, or CircOGDH knockdown and cocultured with hypoxia HBMECs (Figure 4D). CircOGDH levels in sEV were analyzed, showing an increase after H/R with or without CircOGDH overexpression but a decrease with GW4869 treatment or CircOGDH knockdown (Figure 4D). When these sEVs were entered into HBMECs, similar changes were observed in the recipient cells (Figure 4D), indicating that CircOGDH from SH-SY5Y sEVs is taken up by HBMECs, influencing CircOGDH expression.

Next, we investigated the potential effect of CircOGDH regulation on the functionality of HBMECs. We found that sEVs derived from hypoxic SH-SY5Y cells, with or without CircOGDH overexpression, reduced HBMEC apoptosis compared with normoxic HBMECs. This effect was nullified by GW4869-treated sEVs (Figure S14). ECs pretreated with CircOGDH knockdown to eliminate endogenous CircOGDH effects produced similar results in transepithelial electric resistance experiments (Figure 4E and 4F). The results were consistent with CircOGDH regulation directly in HBMECs (Figure S15).

In addition, sEVs from SH-SY5Y cells overexpressing CircOGDH enhanced the migratory capacity of ECs pretreated with sh_CircOGDH AAV transfection, enabling them to cover >65% of the distance during 24 hours; ECs in the H/R group only covered ≈44%. Conversely, sEVs with CircOGDH knockdown exhibited a marked reduction in migratory ability, covering only about 14% of the distance (Figure S16).

We also examined whether sEVs carrying CircOGDH could maintain TJ protein levels in ECs. To highlight the significance of CircOGDH, sEVs isolated from SH-SY5Y cells with CircOGDH knockdown or overexpression were introduced to HBMECs after H/R, and we observed changes in ZO-1 and occludin expression levels. ZO-1 expression in the OE_CircOGDH group was ≈12% higher than in the H/R group (Figure S17A and S17B), while occludin expression was roughly 20% higher (Figure S17A and S17C), with corresponding fluorescence images (Figure S18). Claudin-5 expression also increased by over 10% (Figure S17A and S17D). These results suggest that sEVs overexpressing CircOGDH can partially restore HBMEC migratory function and TJ protein expression.

CircOGDH Regulates the Expression of Its Downstream Protein COL4A4 in Neurons and ECs After H/R

Our previous research identified COL4A4 as a key downstream protein in the CircOGDH neuronal pathway.[3] To confirm COL4A4 as the target gene of CircOGDH in ECs after ischemic stroke, we performed RNA-seq analysis comparing control and CircOGDH-overexpressing HBMECs. This analysis identified 328 significantly upregulated genes (Figure 5A; log2-fold change >2). The Gene Ontology and Kyoto Encyclopedia of Genes and Genomes pathway enrichment analysis revealed that most genes were associated with the collagen-containing extracellular matrix pathway (Figure S19). COL4A4 emerged as a key gene in this pathway, with a 6.9-fold increase in expression, demonstrating consistent

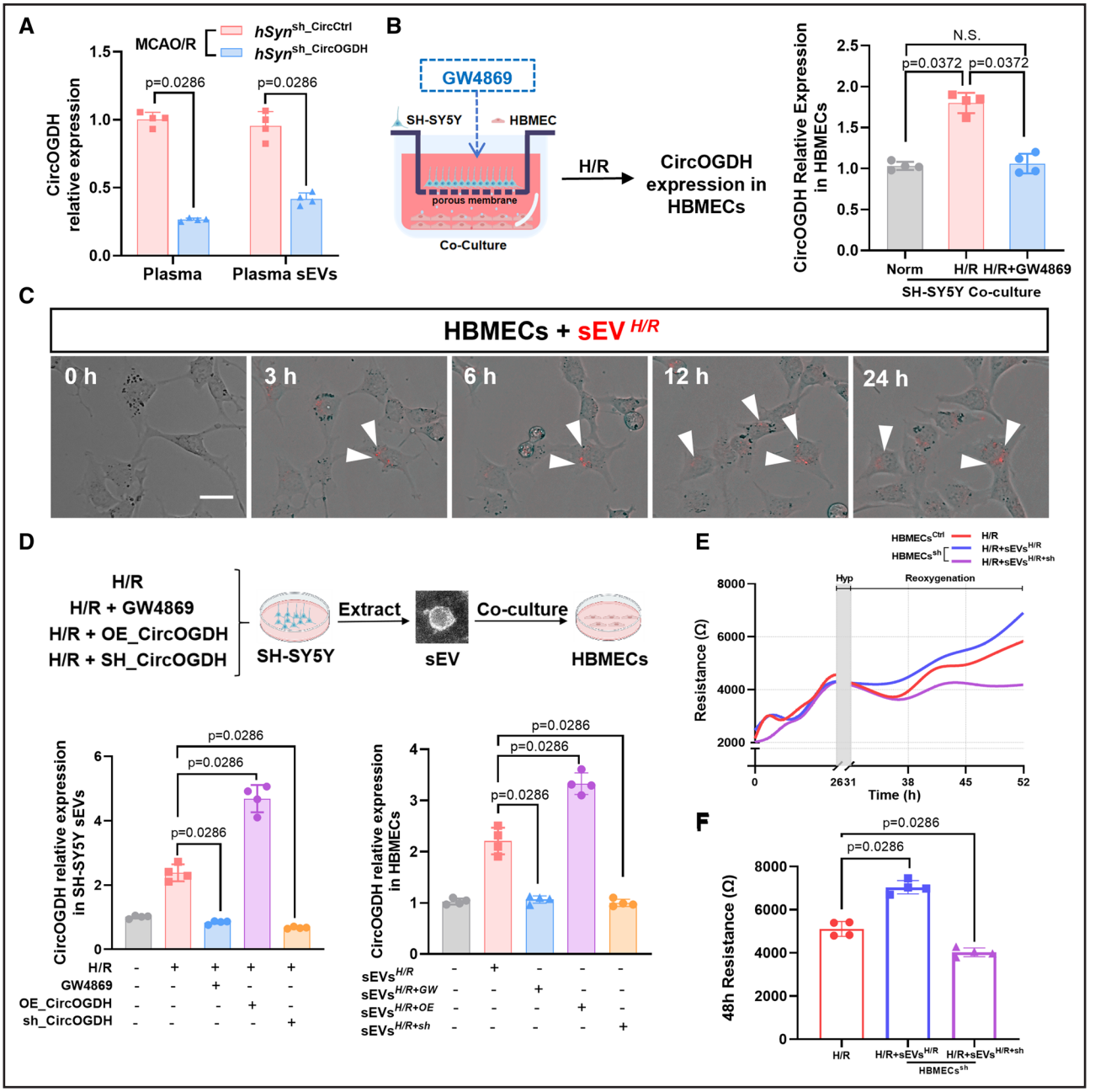

Figure 4. Neuronal circular RNA originating from oxoglutarate dehydrogenase (CircOGDH) modulates human brain microvascular endothelial cell (HBMEC) function after hypoxia/reoxygenation (H/R) by influencing HBMEC CircOGDH levels through small extracellular vesicles (sEVs).

A, Quantitative reverse transcription polymerase chain reaction analysis of CircOGDH levels in mouse plasma or plasma sEVs (n=4). **B**, Schematic of the in vitro blood-brain barrier (BBB) model. Created in BioRender. SH-SY5Y cells were seeded on the inside of collagen-coated 0.4-µm pore poly-(tetrafluoroethylene; PTFE) membrane Transwell inserts and allowed to adhere. HBMECs were seeded in the bottom dishes. Quantitative reverse transcription polymerase chain reaction was performed for CircOGDH levels in cocultured HBMECs with or without GW4869 (exosome inhibitor) treatment in SH-SY5Y cells (n=4). **C**, Live cell workstation used to observe the internalization of PKH26-labeled SH-SY5Y H/R sEVs into HBMECs at different time points. Scale bar, 20 µm. **D**, Schematic: sEVs from SH-SY5Y cells treated under different conditions were extracted and added to the culture medium of HBMECs for coincubation. sEVs from SH-SY5Y cells treated with H/R ($sEV^{H/R}$), H/R+GW4869 ($sEV^{H/R+GW}$), H/R+OE_CircOGDH ($sEV^{H/R+OE}$), or H/R+sh_CircOGDH ($sEV^{H/R+sh}$) were extracted, and CircOGDH levels in the sEVs were measured. sEVs from different sEVs were added to HBMECs for coincubation, and CircOGDH expression levels in HBMECs were measured (n=4). **E** and **F**, Transepithelial electric resistance (TEER) of HBMECs treated with different sEVs during reoxygenation (n=4). $sEV^{H/R}$: sEV from primary neurons cell after hypxia/reoxygenation; $sEV^{H/R}$+sh: sEV from primary neurons under hypxia/reoxygenation after sh_CircOGDH treatment. Data are presented as means±SD; the Mann-Whitney *U* test (**B**, **D**, **E**, and **F**) was used.

 Stroke. 2025;56:1569–1580. DOI: 10.1161/STROKEAHA.124.048446

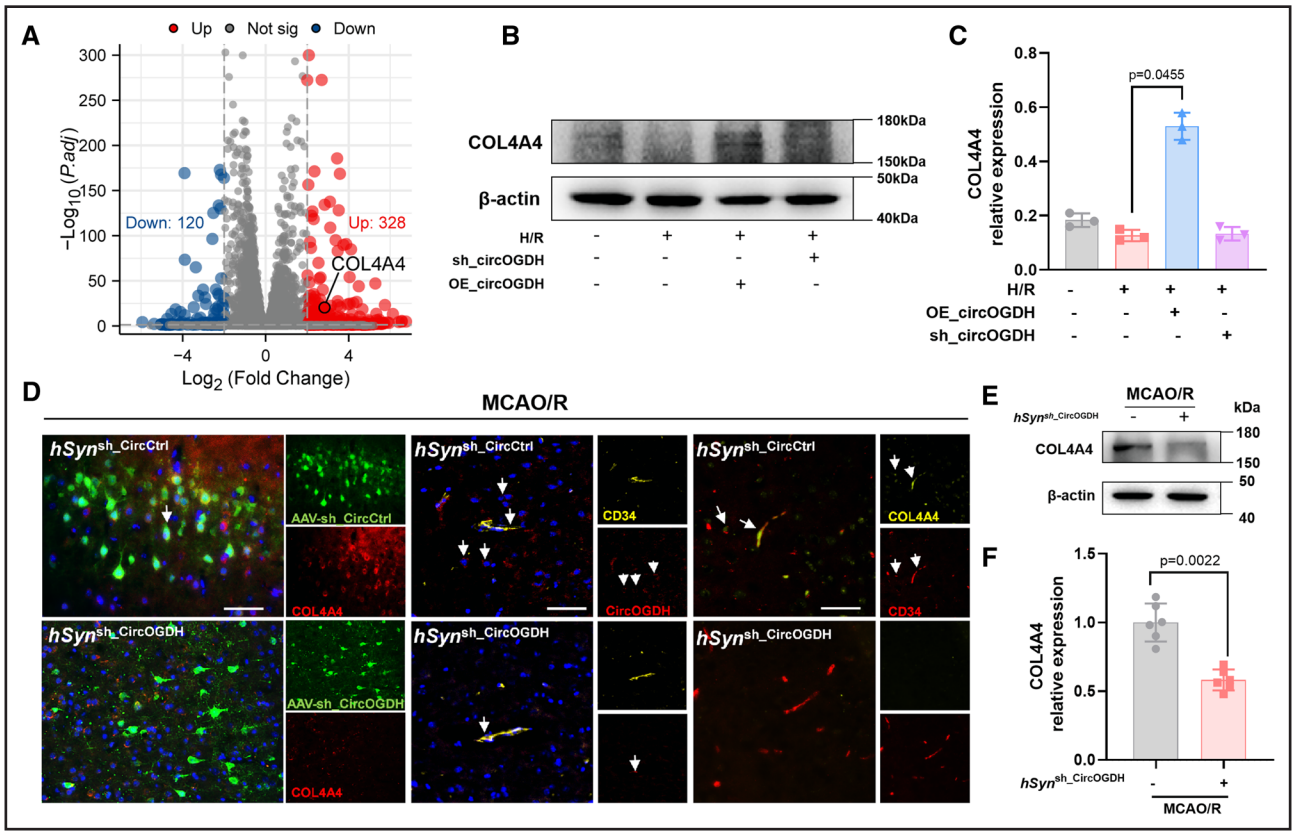

Figure 5. Circular RNA originating from oxoglutarate dehydrogenase (CircOGDH) regulates COL4A4 (collagen type IV alpha 4) expression in neurons and endothelial cells (ECs).

A, Volcano plots showing differentially expressed genes (DEGs) in hypoxic human brain microvascular endothelial cells (HBMECs) transfected with either OE_CircCtrl or OE_CircOGDH (log_2-fold change >2). **B** and **C**, Representative image and statistical analysis of the Western blot for COL4A4 expression in HBMECs (n=3) after transfection with OE_CircOGDH or sh_CircOGDH. **D**, Representative images showing COL4A4 (red) staining in mouse brain sections, with green fluorescence indicating $hSyn^{sh\_CircCtrl}$ or $hSyn^{sh\_CircOGDH}$ virus (**left**). Colocalization of CircOGDH (red) with CD34 (yellow) in ECs of the mouse brain (**middle**) and COL4A4 (yellow) with CD34 (red) in ECs (**right**). Scale bar, 200 μm. **E** and **F**, Representative image and statistical analysis of the Western blot for COL4A4 in penumbra tissue (PEN) of the mouse brain (n=6). Data are presented as means±SD; the Kruskal-Wallis test (**C**) and the Mann-Whitney *U* test (**F**) were used.

biological reproducibility across 3 replicates (Figure S20). The Western blot analysis confirmed COL4A4 upregulation in CircOGDH-overexpressing HBMECs (Figure 5B and 5C). We also observed COL4A4 localization in brain tissue from patients with AIS+HT, colocalized with CD31 (Figure S21). In MCAO/R mice, neuronal CircOGDH knockdown ($hSyn^{sh\_CircOGDH}$) reduced COL4A4 expression in brain penumbra tissue (Figure 5D). Colocalization of CircOGDH and CD34 was significantly reduced in the $hSyn^{sh\_CircOGDH}$ group compared with the $hSyn^{sh\_CircCtrl}$ group (Figure 5D). COL4A4 expression followed the same trend as CircOGDH expression (Figure 5E and 5F).

To further validate the role of neuronal sEVs delivering CircOGDH to regulate COL4A4 in ECs, we established an in vitro neurovascular unit interaction model using a coculture system. The Western blot analysis revealed a delayed increase in COL4A4 expression in HBMECs, peaking at 24 hours after reoxygenation (Figure S22), while CircOGDH levels in recipient HBMECs peaked earlier, following 3 hours of hypoxia treatment in cocultured SH-SY5Y cells. As COL4A4 levels increased, TJ proteins also showed increased expression after 24 and 48 hours of reoxygenation. Blocking sEV release with GW4869 in the Transwell system suppressed CircOGDH expression in HBMECs (Figure 4B) and inhibited COL4A4 expression (Figure S23). These dynamic changes in CircOGDH and COL4A4 over time suggest that neuronal CircOGDH is transported to ECs, regulating COL4A4 expression.

Regulation of HBMEC Function by CircOGDH Is Mediated Through COL4A4

We further verified the influence of the CircOGDH/COL4A4 axis on HBMEC function during hypoxia. While TJ protein expression in ECs decreased after H/R stimulation, it increased with CircOGDH overexpression (Figure S24) but could not restore TJ proteins when COL4A4 was knocked down. Conversely, overexpression of COL4A4 maintained TJ protein levels even when CircOGDH was inhibited in hypoxic ECs (Figure 6A and

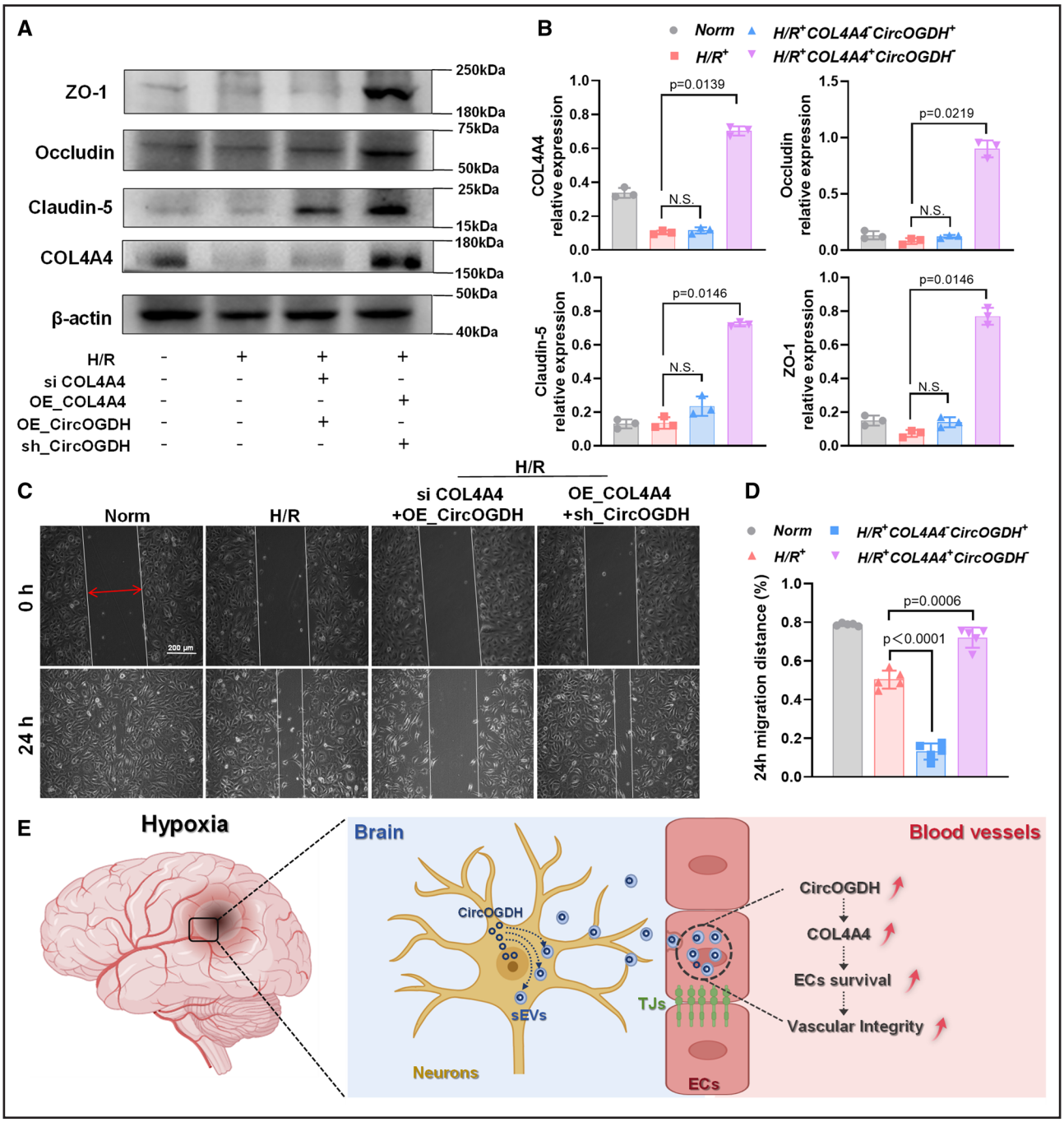

Figure 6. Regulation of human brain microvascular endothelial cell (HBMEC) function by circular RNA originating from oxoglutarate dehydrogenase (CircOGDH) is mediated through COL4A4 (collagen type IV alpha 4).
A and **B**, Representative image and statistical analysis of the Western blot for ZO-1/occludin/claudin-5/COL4A4 expression in normoxic and hypoxic HBMECs after transfection with OE_CircOGDH, siCOL4A4, or sh_CircOGDH and OE_COL4A4 (n=3). **C** and **D**, Migration of HBMECs in a scratch assay. Quantitative analysis of the distance covered by HBMECs (**D**; n=6). Data are presented as means±SD; the Kruskal-Wallis test (**B**) and 1-way ANOVA with the Dunnett multiple comparisons test (**D**) were used. **E**, Schematic diagram illustrating the neuronal regulation of endothelial cells (ECs) via the release of small extracellular vesicles (sEVs). Created in BioRender.

6B). Migration assays yielded similar results, emphasizing CircOGDH's regulatory role through COL4A4 in EC function during hypoxia (Figure 6C and 6D). These findings suggest that CircOGDH, delivered by hypoxic neurons via sEVs, enhances EC function and morphology by increasing COL4A4 expression (Figure 6E).

DISCUSSION

This study delves into the role of CircOGDH, a circular RNA in penumbra neurons, concerning HT in AIS. Elevating hypoxic neuronal sEVs increases CircOGDH levels in ECs along with the expression of its downstream

Stroke. 2025;56:1569–1580. DOI: 10.1161/STROKEAHA.124.048446

protein COL4A4, enhancing EC function and TJ protein expression. This underscores a novel regulatory mechanism in stroke pathology.

We observed lower CircOGDH expression in hemorrhagic patients with AIS compared with nonhemorrhagic patients with AIS, with a negative correlation between CircOGDH levels and hematoma volume in patients with HT. This suggests a potential protective role of CircOGDH against HT in the BBB after AIS. Measuring CircOGDH levels could serve as a valuable biomarker for predicting hemorrhagic risk in patients with AIS, guiding therapeutic decisions to mitigate risk factors associated with HT in the clinical setting.

The delivery of CircOGDH from hypoxic neurons influences BBB integrity for several reasons. Targeted knockdown of neuronal CircOGDH in mouse models exacerbated BBB permeability, disrupting TJs crucial for the barrier properties of the BBB and leading to increased vascular permeability.[18,19] Because CircOGDH regulates COL4A4 expression in ECs, it indicates a strategy for enhancing the extracellular matrix and maintaining TJ proteins in ECs to preserve vascular wall integrity.[20–22] In addition, the interaction of CircOGDH with endothelial caveolae, marked by Cav-1, suggests its role in modulating BBB permeability by regulating endothelial transcytosis and endocytosis, contributing to BBB integrity after a stroke.[23–25] In addition, the lower levels of CircOGDH in the ischemic brain may facilitate BBB disruption and subsequent HT following stroke. As the BBB becomes changed, CircOGDH can more easily leak into the bloodstream, increasing its levels in plasma. Future studies could explore the mechanisms of CircOGDH in plasma related to BBB disruption or changes in endothelial transport.

Neuronal sEVs carrying CircOGDH impact ECs, highlighting the importance of ECs in neuron-vascular communication. Recently, brain cell-derived sEVs have been detected in peripheral blood and identified as a biomarker for several neurodegenerative diseases,[26–28] suggesting a targeting of ECs by neuronal cell-derived sEVs.[29,30] Increased neuronal activity leads to heightened sEV release,[8,31] especially as vascularization and mature BBB formation occur concurrently in the developing brain.[11,32,33] Investigating how neuronal sEVs carrying CircOGDH affect neurovascular units in brain development could yield valuable insights.

We elucidated the biological process of hypoxic neurons releasing CircOGDH to the BBB, facilitating molecular communication with the blood. Administering sEVs containing CircOGDH via peripheral blood may be a therapeutic strategy for maintaining BBB integrity under hypoxic conditions. Future research should aim to elucidate the specific molecules within sEVs and their impact on neurovascular communication.

A limitation of this study is our focus on the acute phase of stroke-induced BBB damage. Longitudinal research on CircOGDH levels throughout stroke progression and recovery phases, as well as its impact on neurovascular coupling, is necessary for a comprehensive understanding.

In conclusion, we discovered the vital role of neuronal CircOGDH under hypoxia in influencing ECs through sEVs, crucial for COL4A4 expression in ECs and preserving BBB integrity. Pharmacologically, developing a neuronal-specific CircOGDH inhibitor for hypoxic neurons and an endothelial-targeted CircOGDH agonist (Figure 6E) could be beneficial in AIS treatment. Alternatively, modulating hypoxia-induced neuronal sEVs release targeting ECs may offer a rational therapeutic approach. Our findings shed light on neurovascular interactions in hypoxia, emphasizing the significance of neuronal sEVs in regulating cerebral vascular diseases.

ARTICLE INFORMATION

Received July 06, 2024; final revision received January 28, 2025; accepted February 21, 2025.

Affiliations

Department of Neurology and Stroke Center (W.C., Y.W., Y.L., X.S., M.K., D.D., J. Zang, A.X., D.L.), Clinical Neuroscience Institute (W.C., Y.W., Y.L., X.S., M.K., D.D., J. Zang, A.X., D.L.), and Key Laboratory of Guangzhou Basic and Translational Research of Pan-Vascular Diseases (W.C., Y.W., Y.L., X.S., M.K., D.D., J. Zang, A.X., D.L.), The First Affiliated Hospital of Jinan University, Guangzhou, China. Department of Neurology, Beijing Tiantan Hospital, Capital Medical University, China (W.C.). China National Clinical Research Center for Neurological Diseases, Beijing (W.C.). Department of Neurology, Sun Yat-sen Memorial Hospital, Sun Yat-sen University, Guangzhou, China (H.M.). Department of Neurology, The First People's Hospital of Foshan, China (J. Zang). Department of Neurology, The Affiliated Shunde Hospital of Jinan University, Foshan, China (J. Zhu).

Acknowledgments

The authors gratefully thank the patients for their participation in this study. The authors acknowledge the Central Laboratory of Basic Medical College, Department of Animal Magnetic Resonance Research Center of the First Affiliated Hospital of Jinan University, for providing the required equipment used in this study.

Sources of Funding

This work was supported by grants from the National Natural Science Foundation of China (82271304, 81801150, 82171316, 82401525, and 82401561), the Guangdong TeZhi Plan (0720240214), the Natural Science Foundation of Guangdong Province (2018A0303130182, 2020A1515010279, and 2022A1515012311), the Science and Technology Projects in Guangzhou (2025A04J6829, 202201010127, and 2023A03J1021), the Science and Technology Program of Guangzhou: Key Laboratory of Guangzhou Basic and Translational Research of Pan-Vascular diseases (202201020042), the Young Talent Support Project of Guangzhou Association for Science and Technology (QT-2023-024), the Guangdong Basic and Applied Basic Research Foundation (2025B1515020086, 2023A1515111085), the China Postdoctoral Science Foundation (2023M741383). The Sun Yat-sen University Hundreds of Talent Program (1320324001), and the Fundamental Research Funds for the Central Universities, Sun Yat-sen University (24qnpy309).

Disclosures

None.

Supplemental Material

Supplemental Methods
Tables S1–S9
Figure S1–S24

REFERENCES

1. Ghozy S, Reda A, Varney J, Elhawary AS, Shah J, Murry K, Sobeeh MG, Nayak SS, Azzam AY, Brinjikji W, et al. Neuroprotection in acute ischemic stroke: a battle against the biology of nature. *Front Neurol.* 2022;13:870141. doi: 10.3389/fneur.2022.870141

2. Goyal M, Menon BK, van Zwam WH, Dippel DW, Mitchell PJ, Demchuk AM, Davalos A, Majoie CB, van der Lugt A, de Miquel MA, et al; HERMES Collaborators. Endovascular thrombectomy after large-vessel ischaemic stroke: a meta-analysis of individual patient data from five randomised trials. *Lancet*. 2016;387:1723–1731. doi: 10.1016/S0140-6736(16)00163-X
3. Liu Y, Li Y, Zang J, Zhang T, Li Y, Tan Z, Ma D, Zhang T, Wang S, Zhang Y, et al. CircOGDH is a penumbra biomarker and therapeutic target in acute ischemic stroke. *Circ Res*. 2022;130:907–924. doi: 10.1161/CIRCRESAHA.121.319412
4. Walther J, Kirsch EM, Hellwig L, Schmerbeck SS, Holloway PM, Buchan AM, Mergenthaler P. Reinventing the penumbra - the emerging clockwork of a multi-modal mechanistic paradigm. *Transl Stroke Res*. 2023;14:643–666. doi: 10.1007/s12975-022-01090-9
5. del Zoppo GJ, Sharp FR, Heiss WD, Albers GW. Heterogeneity in the penumbra. *J Cereb Blood Flow Metab*. 2011;31:1836–1851. doi: 10.1038/jcbfm.2011.93
6. Puig B, Brenna S, Magnus T. Molecular communication of a dying neuron in stroke. *Int J Mol Sci*. 2018;19:2834. doi: 10.3390/ijms19092834
7. Dirnagl U, Iadecola C, Moskowitz MA. Pathobiology of ischaemic stroke: an integrated view. *Trends Neurosci*. 1999;22:391–397. doi: 10.1016/s0166-2236(99)01401-0
8. Schnatz A, Muller C, Brahmer A, Kramer-Albers EM. Extracellular vesicles in neural cell interaction and CNS homeostasis. *FASEB Bioadv*. 2021;3:577–592. doi: 10.1096/fba.2021-00035
9. Filannino FM, Panaro MA, Benameur T, Pizzolorusso I, Porro C. Extracellular vesicles in the central nervous system: a novel mechanism of neuronal cell communication. *Int J Mol Sci*. 2024;25:1629. doi: 10.3390/ijms25031629
10. Stackhouse TL, Mishra A. Neurovascular coupling in development and disease: focus on astrocytes. *Front Cell Dev Biol*. 2021;9:702832. doi: 10.3389/fcell.2021.702832
11. Kaplan L, Chow BW, Gu C. Neuronal regulation of the blood-brain barrier and neurovascular coupling. *Nat Rev Neurosci*. 2020;21:416–432. doi: 10.1038/s41583-020-0322-2
12. Reymond S, Vujic T, Sanchez JC. Neurovascular unit-derived extracellular vesicles: from their physiopathological roles to their clinical applications in acute brain injuries. *Biomedicines*. 2022;10:2147. doi: 10.3390/biomedicines10092147
13. Tilson HA, Schroeder JC. Reporting of results from animal studies. *Environ Health Perspect*. 2013;121:A320–A321. doi: 10.1289/ehp.1307676
14. Knowland D, Arac A, Sekiguchi KJ, Hsu M, Lutz SE, Perrino J, Steinberg GK, Barres BA, Nimmerjahn A, Agalliu D. Stepwise recruitment of transcellular and paracellular pathways underlies blood-brain barrier breakdown in stroke. *Neuron*. 2014;82:603–617. doi: 10.1016/j.neuron.2014.03.003
15. Mendes RT, Nguyen D, Stephens D, Pamuk F, Fernandes D, Hasturk H, Van Dyke TE, Kantarci A. Hypoxia-induced endothelial cell responses - possible roles during periodontal disease. *Clin Exp Dent Res*. 2018;4:241–248. doi: 10.1002/cre2.135
16. Xue Y, Wang X, Wan B, Wang D, Li M, Cheng K, Luo Q, Wang D, Lu Y, Zhu L. Caveolin-1 accelerates hypoxia-induced endothelial dysfunction in high-altitude cerebral edema. *Cell Commun Signal*. 2022;20:160. doi: 10.1186/s12964-022-00976-3
17. Lossinsky AS, Shivers RR. Structural pathways for macromolecular and cellular transport across the blood-brain barrier during inflammatory conditions. Review. *Histol Histopathol*. 2004;19:535–564. doi: 10.14670/HH-19.535
18. Robles-Osorio ML, Sabath E. Tight junction disruption and the pathogenesis of the chronic complications of diabetes mellitus: a narrative review. *World J Diabetes*. 2023;14:1013–1026. doi: 10.4239/wjd.v14.i7.1013
19. Aghajanian A, Wittchen ES, Allingham MJ, Garrett TA, Burridge K. Endothelial cell junctions and the regulation of vascular permeability and leukocyte transmigration. *J Thromb Haemost*. 2008;6:1453–1460. doi: 10.1111/j.1538-7836.2008.03087.x
20. Komarova YA, Kruse K, Mehta D, Malik AB. Protein interactions at endothelial junctions and signaling mechanisms regulating endothelial permeability. *Circ Res*. 2017;120:179–206. doi: 10.1161/CIRCRESAHA.116.306534
21. Forouzandeh M, Mostafavi H, Ghasemloo E, Mohammadi P, Hosseini M, Eskandari M. Increased expression of tight junction proteins and blood-brain barrier integrity in MCAO rats following injection of miR-149-5p. *Int J Mol Cell Med*. 2022;11:223–235. doi: 10.22088/IJMCM.BUMS.11.3.223
22. Davis GE, Senger DR. Endothelial extracellular matrix: biosynthesis, remodeling, and functions during vascular morphogenesis and neovessel stabilization. *Circ Res*. 2005;97:1093–1107. doi: 10.1161/01.RES.0000191547.64391.e3
23. Dalton CM, Schlegel C, Hunter CJ. Caveolin-1: a review of intracellular functions, tissue-specific roles, and epithelial tight junction regulation. *Biology (Basel)*. 2023;12:1402. doi: 10.3390/biology12111402
24. Shu Y, Jin S. Caveolin-1 in endothelial cells: a potential therapeutic target for atherosclerosis. *Heliyon*. 2023;9:e18653. doi: 10.1016/j.heliyon.2023.e18653
25. Frank PG, Woodman SE, Park DS, Lisanti MP. Caveolin, caveolae, and endothelial cell function. *Arterioscler Thromb Vasc Biol*. 2003;23:1161–1168. doi: 10.1161/01.ATV.0000070546.16946.3A
26. Li Z, Wang X, Wang X, Yi X, Wong YK, Wu J, Xie F, Hu D, Wang Q, Wang J, et al. Research progress on the role of extracellular vesicles in neurodegenerative diseases. *Transl Neurodegener*. 2023;12:43. doi: 10.1186/s40035-023-00375-9
27. Kumar A, Su Y, Sharma M, Singh S, Kim S, Peavey JJ, Suerken CK, Lockhart SN, Whitlow CT, Craft S, et al. MicroRNA expression in extracellular vesicles as a novel blood-based biomarker for Alzheimer's disease. *Alzheimers Dement*. 2023;19:4952–4966. doi: 10.1002/alz.13055
28. Sproviero D, Gagliardi S, Zucca S, Arigoni M, Giannini M, Garofalo M, Fantini V, Pansarasa O, Avenali M, Ramusino MC, et al. Extracellular vesicles derived from plasma of patients with neurodegenerative disease have common transcriptomic profiling. *Front Aging Neurosci*. 2022;14:785741. doi: 10.3389/fnagi.2022.785741
29. Zhang L, Li C, Huang R, Teng H, Zhang Y, Zhou M, Liu X, Fan B, Luo H, He A, et al. Cerebral endothelial cell derived small extracellular vesicles improve cognitive function in aged diabetic rats. *Front Aging Neurosci*. 2022;14:926485. doi: 10.3389/fnagi.2022.926485
30. Yue KY, Zhang PR, Zheng MH, Cao XL, Cao Y, Zhang YZ, Zhang YF, Wu HN, Lu ZH, Liang L, et al. Neurons can upregulate Cav-1 to increase intake of endothelial cells-derived extracellular vesicles that attenuate apoptosis via miR-1290. *Cell Death Dis*. 2019;10:869. doi: 10.1038/s41419-019-2100-5
31. Ransom LS, Liu CS, Dunsmore E, Palmer CR, Nicodemus J, Ziomek D, Williams N, Chun J. Human brain small extracellular vesicles contain selectively packaged, full-length mRNA. *Cell Rep*. 2024;43:114061. doi: 10.1016/j.celrep.2024.114061
32. Aazmi A, Zhou H, Lv W, Yu M, Xu X, Yang H, Zhang YS, Ma L. Vascularizing the brain in vitro. *iScience*. 2022;25:104110. doi: 10.1016/j.isci.2022.104110
33. Zlokovic BV. The blood-brain barrier in health and chronic neurodegenerative disorders. *Neuron*. 2008;57:178–201. doi: 10.1016/j.neuron.2008.01.003